ELSEVIER

Journal of Crystal Growth 164 (1996) 34–39

JOURNAL OF CRYSTAL GROWTH

Real-time optical monitoring of $Ga_xIn_{1-x}P$ and GaP heteroepitaxy on Si under pulsed chemical beam conditions

N. Dietz [a,b,*], U. Rossow [a], D.E. Aspnes [a], K.J. Bachmann [b,c]

[a] *Department of Physics, North Carolina State University, Raleigh, North Carolina 27695, USA*
[b] *Department of Materials Science, North Carolina State University, Raleigh, North Carolina 27695, USA*
[c] *Department of Chemical Engineering, North Carolina State University, Raleigh, North Carolina 27695, USA*

Abstract

In this paper we describe the combined application of p-polarized reflectance spectroscopy (PRS), reflectance difference spectroscopy (RDS), and laser light scattering (LLS) to investigate the growth of $Ga_xIn_{1-x}P$/GaP on Si by pulsed chemical beam epitaxy (PCBE) with tertiarybutylphosphine, triethylgallium, and trimethylindium precursors. The pulsed supply of chemical precursors causes a periodic alteration of the surface composition, which is observed as corresponding periodicity (fine structure) in the RD and PRS signals, confirming the high sensitivity of both methods to surface chemistry during the entire growth process. This fine structure is modeled under conditions where the surface chemistry periodically alternates between a four-layer stack (ambient/surface layer/film/substrate) and a three layer stack (ambient/film/substrate) description with a corresponding alteration in the optical response of the PRS and RD signals. RD spectra are used to estimate the surface reconstruction of the layers. LLS provides information about the surface topography and thus the evolution of surface roughness, which is especially important during nucleation.

1. Introduction

The application of optical techniques to the real-time monitoring of deposition and etching is attractive because of their non-invasive character. A variety of methods, such as spectral-resolved normal incidence reflectance spectroscopy (NRIS) [1] and pyrometric interferometry (PI) [2] have been successfully applied to monitor the growth rate and the composition of the growing film in industrial applications, which require low cost and robust performance. In order to gain a higher sensitivity to surface- and interface-related growth properties, alternative in-situ optical methods such as reflectance difference spectroscopy (RDS) [3–5], surface photo-absorption (SPA) [6,7] and spectral ellipsometry (SE) [3,8] have been developed. Recently, we added to these methods a real-time optical monitoring technique, p-polarized reflectance spectroscopy (PRS), which achieves both (i) high sensitivity to the surface kinetics under quasi-steady-state growth conditions and (ii) the capability of monitoring film thickness and optical properties with submonolayer resolution [9–16].

PRS measures the p-polarized reflectance $R_p = r_p r_p^*$ at an angle of incidence near to the Brewster angle φ_B of the substrate (pseudo-Brewster angle for an absorbing media). For the silicon/vacuum interface in the weak absorbing spectral regime ($\lambda > 500$ nm) the p-polarized reflectance component is of the

* Corresponding author.

0022-0248/96/$15.00 Copyright © 1996 Elsevier Science B.V. All rights reserved
SSDI 0022-0248(95)01018-1

order of 10^{-4}. Therefore, the reflected intensity is a sensitive function of any changes of the dielectric function of silicon surface, which may be due to temperature-induced changes in the dielectric function of the substrate, surface roughening, surface chemical modifications, or overgrowth by a thin film having a dielectric function that differs from that of the Si substrate. The LLS intensity is detected with a photomultiplier tube (PMT) located 45° away from the plane of incidence. RDS measures the optical anisotropy of the sample, which is normally dominated by that between the [$\bar{1}$10] and [110] principal axes of the (001) surface. The configuration and approach have been described in detail elsewhere [5]. Our spectral range is 1.5 to 5.5 eV. The light enters the chamber through a nominally strain-free quartz window [17]. Corrections of residual strain effects in the window were unnecessary.

Here, we examine the heteroepitaxial growth of GaP on Si substrates through simultaneous measurements by single-wavelength PRS and LLS (HeNe laser source, $\lambda = 6328$ Å) and RDS under pulsed chemical beam epitaxy conditions specifically, surfaces are exposed to pulsed ballistic beams of tertiarybutyl phosphine [TBP $(C_4H_9)PH_2$], triethylgallium [TEG, $Ga(C_2H_5)_3$] and trimethylindium [TMI, $In(CH_3)_3$] at sample temperature from 350 to 400°C to accomplish nucleation and overgrowth of the silicon by an epitaxial GaP film and in the subsequent heteroepitaxial growth of $Ga_xIn_{1-x}P$ on GaP. The Si(001) substrates were vicinally cut 6° toward (011). Both these and the Si(113) substrates are boron-doped with resistivities from 1 to 10 Ω · cm. Preparation consisted of an RCA clean followed by a DI-H_2O rinse, a final HF dip and a short DI-H_2O rinse. The samples are then transferred via a load lock into the growth chamber. This treatment produces a (1 × 1) hydrogen-terminated Si(001) surface as verified by RHEED. The flows of precursors and hydrogen are established by mass flow controllers and are directed by computer-controlled 3-way valves to either the reactor chamber or a separately pumped bypass chamber. This allows the substrate to be exposed sequentially to the individual pulses of the precursor molecules with no overall pressure variations. The switching of the sources is synchronized with the data acquisition of the PRS and LLS signals to correlate changes in the reflected intensity to chemically induced changes in the surface condition and/or the optical properties of the growing film. Typical growth rates under the present conditions are about 1 Å/s. Further experimental details are given in a previous publication [13].

2. Fine structure model consideration

As shown in previous publications [9–16], upon heteroepitaxial growth the reflectance $R_p = r_p r_p^*$ shows interference oscillations with increasing film thickness. Under pulsed precursor conditions an additional fine structure in the PR and RD response is observed, which is directly linked to the precursor cycle sequence. For a better understanding of the origin of the fine structure, we use a simplified model that predicts certain features in the fine structure and permit the determination of the imaginary part of the dielectric function associated with the surface reaction layer. This model is based on the four-layer stack shown schematically in Fig. 1. This stack consists of the substrate, the heteroepitaxial film, the surface reaction layer and the ambient. Fresnel's equations for a multilayer stack [13] are used to calculate the changes of the reflectance of p-polarized light as a function of time, assuming homogenous isotropic media. The fine structure in the PRS signal is modeled by a surface reaction layer that is periodically created and removed during the GaP film growth. The precursor sequence that describes the time-dependent exposure of the surface is shown schematically in Fig. 2a. The sequence is schematically linked to the surface reaction layer in

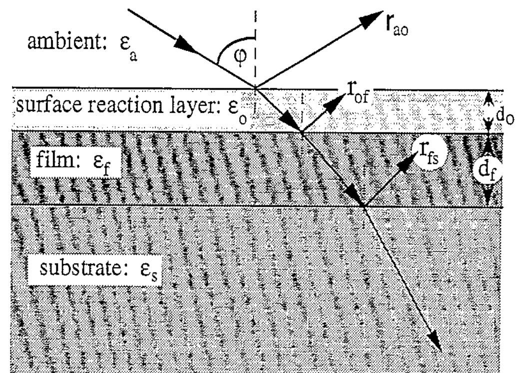

Fig. 1. Schematic representation of a four-layer stack.

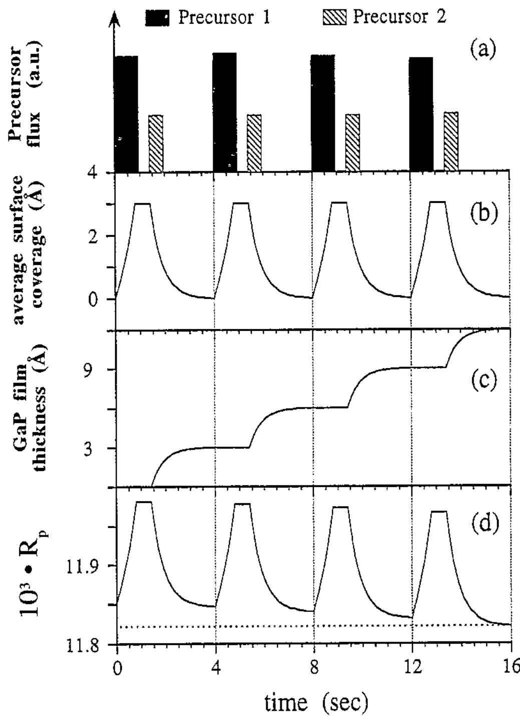

Fig. 2. Model simulations: (a) precursor sequence with #1 and #2 precursor pulses from 0.0–0.8 s and 1.4–1.8 s, respectively; (b) calculated correlated changes in the average thickness of a surface reaction layer; (c) time-dependent increase of the bulk film thickness during the cycle sequence with a growth rate of 3 Å per cycle; (d) calculated changes in the reflectance during the time evolution of the surface layer and bulk film growth processes.

Fig. 2b. The surface layer is assumed to grow during exposure to precursor #1 and to be consumed exponentially during the exposure to precursor #2, which also results in an increase of the thickness of the underlying film as shown schematically in Fig. 2c. The consumption process is modeled through an exponential function with an adjustable decay factor α_{od} that is determined by the #2 precursor flux, the sticking coefficients of the #2 precursor radicals, and the chemical reaction rates for transforming the surface species into the growing film. Note that the elimination of the surface reaction layer by #2 precursor is arbitrary and would not correspond to reality if the #2 precursor decays slowly [14]. With these assumptions we can calculate the changes in the reflectance during the time evolution of the surface layer at $\lambda = 6328$ Å, an angle of incidence $\varphi = 72°$, a Si dielectric function of $\epsilon_{Si} = (15.25, 0.17)$ [18] and a GaP dielectric function of $\epsilon_{GaP} = (11.11, 0.0)$ [19].

The model calculations show that the amplitude of the fine structure changes during the deposition process as a result of its interaction with the interference oscillations. The amplitude increases on the raising flanks of the interference oscillations with a maximum at the top, and then decreases on the falling flanks. The relative locations of these increases and decreases of the fine structure amplitude with respect to the phase of the film interference oscillations strongly depend on the chosen growth conditions, such as the widths and heights of the precursor pulses, their sequence times, and the supply of additional activated hydrogen. A detailed model analysis shows that the thicknesses for which the fine structure almost vanishes coincides with a change in the sign of the optical response to the first precursor pulse of the sequence. This changeover in the sign of the optical response with respect to the fine structure, which we denote as turning point, allows a precise determination of the imaginary part of the dielectric function of the surface layer, ϵ_{O_2} [16].

3. GaP heteroepitaxy on Si

Fig. 3 shows RDS spectra taken during interruptions of the growth of GaP on Si(113) with the

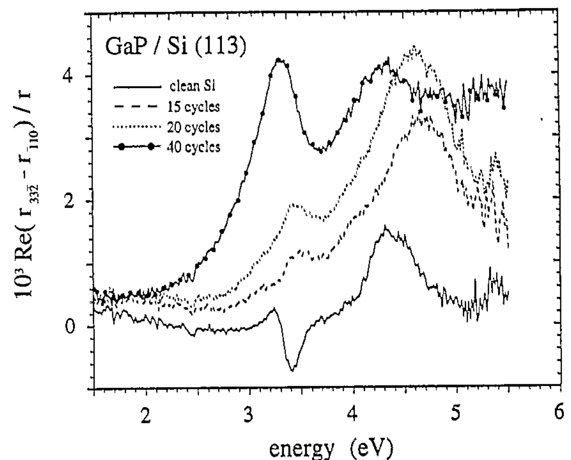

Fig. 3. Evolution of RDS spectra during GaP growth. The sample labeled clean Si is taken with the sample at room temperature; the rest are obtained at 350°C.

substrate at growth temperature and under continuous TBP flow. For comparison the RT RDS spectrum of the clean Si(113) surface is also shown. Two notable features develop in the spectra. The one near 3.4 eV shifts to 3.3 eV and becomes sharper with increasing thickness. The second, near 4.6 eV for small coverages, shifts to lower values for higher coverages finally reaching an energy of 4.3 eV. The spectrum observed after 40 cycles resembles the imaginary part of the dielectric function bulk GaP as discussed in detail in Ref. [20]. Since no features in these spectra appear below 3 eV – contrary to the situations of InP or GaAs homoepitaxy – we assume that the surface is in a phosphorous-rich reconstruction. During the initial stages of deposition, the RD signal cannot be assigned alone because the GaP/Si interface may still contribute. The small spectral range of the lower feature suggests thus.

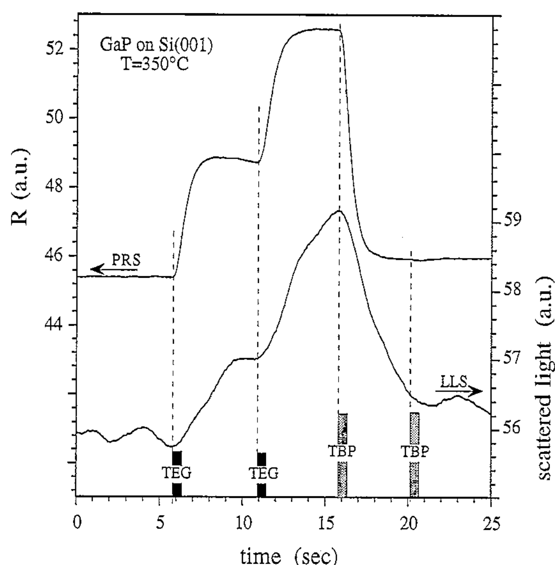

Fig. 4. PRS and LLS responses to individual precursor pulses performed during an interruption of growth at growth temperature.

4. Surface reaction kinetics during quasi-steady-state growth conditions

For more specific information about the time constants of the surface-reaction kinetics, we performed experiments with single pulses of TEG and TBP. As an example, the PRS and LLS responses to individual precursor pulses for a double-pulse experiment, consisting of double TEG and TBP pulses on the raising flank of the PR interference oscillation are shown in Fig. 4. The experiments are performed under quasi-steady-state GaP growth conditions during an interruption of growth. After a 0.5 s exposure of the surface to TEG, the TEG fragments decompose on the surface resulting in an increase in the PRS signal and a delayed increase in the LLS intensity, which is related to the Ga cluster formation. After the second TEG pulse the PRS signal increases as a response to an increased surface reaction layer, but stays constant during the further waiting period. The slight decrease of the PRS signal during the waiting period after the first TEG pulse can be related to the partial reaction of the TEG fragments with remaining phosphorus on the surface, which reduces the thickness of the surface reaction layer. This decrease is not observed after the second TEG pulse. The optical response to the first TBP pulse is significant. First, the PRS signal decreases exponentially and levels off at a slightly increased reflectance baseline due to the increase of the GaP film thickness. Secondly, the LLS intensity decreases slowly indicating a smoothing of the GaP surface. For the second TBP exposure no further changes in the PRS signal are observed.

5. $Ga_xIn_{1-x}P$ heteroepitaxy on GaP

The PRS, RD and LLS responses during a transition from GaP to $Ga_xIn_{1-x}P$ heteroepitaxial growth are shown in Fig. 5. The evolution of the RD transient is monitored at 2.6 eV. The precursor sequence during GaP growth consists of a TBP pulse from 0.0–0.8 s and a TEG pulse from 1.5–1.9 s for a total cycle time of 3 s. Upon changing from GaP to $Ga_xIn_{1-x}P$ growth we add a TMI pulse from 4.5–4.9 s for a total cycle time of 6 s. Fig. 6 shows the optical response to the last GaP sequence and the first three $Ga_xIn_{1-x}P$ sequences in more detail. The period of the response to the GaP precursor sequence remains unchanged in the PRS signal, while the RD time evolution is affected by the first TBP/TMI cycle. After approximately five $Ga_xIn_{1-x}P$ cycles a modified RD signal with a 6 s period and a reduced amplitude is observed. The rising edge of the RD

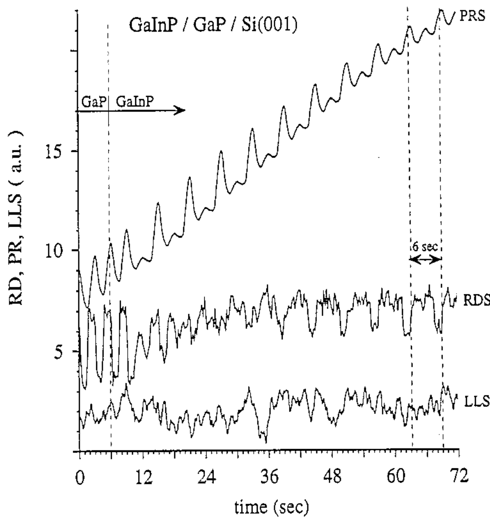

Fig. 5. Traces of PR and RD signals for the heteroepitaxial growth of $Ga_xIn_{1-x}P$ on GaP. The fluxes of TBP, TEG and TMI are 1, 0.06 and 0.03 sccm, respectively.

signal is normally correlated with the onset of the TEG pulse and the falling edge with the onset of TBP. With respect to the TBP pulse the response is

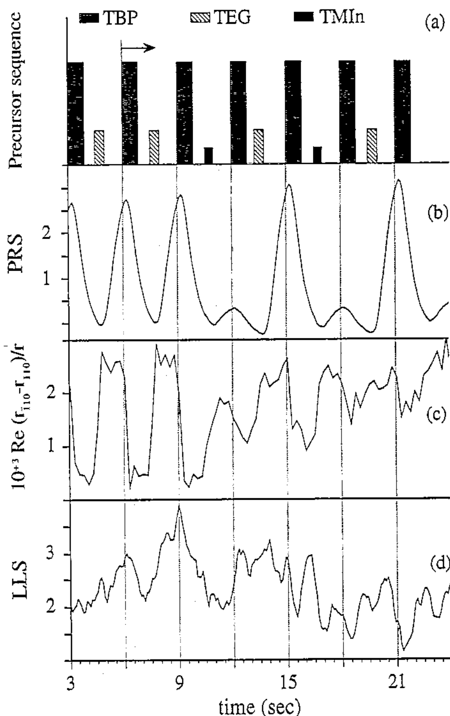

Fig. 6. Enlarged traces of PRS, RD, and LLS signals during the transition of GaP to $Ga_xIn_{1-x}P$.

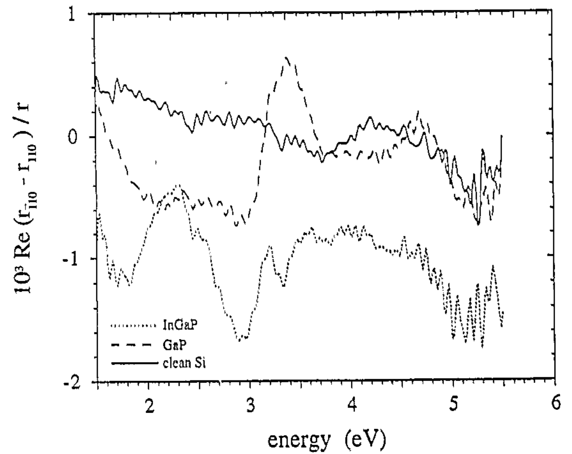

Fig. 7. Comparison of RD spectra of $Ga_xIn_{1-x}P$ and GaP on Si.

changed to a rising transient, while under GaP growth conditions the response is a falling transient. After prolonged growth no response of the RD signal to the precursor pulse is observable. Therefore, the surface must be highly loaded with group V elements such that the surface immediately returns to the upper position.

Fig. 7 shows the evolution of RD spectra taken during growth interruptions of $Ga_xIn_{1-x}P/GaP$ heteroepitaxy on vicinal Si(001). On this scale the spectrum of the clean Si(001) substrate is nearly featureless. For Si(113) the spectrum for the GaP layer shows two features. One is near 3.4 eV the other near 4.2 eV. The absolute values are much smaller than for Si(113). We attribute thus to the presence of anti-phase-domains (APD) in the vicinal Si(001) layer that partly cancel the signal [20].

In conclusion, we have applied PRS, RDS, and LLS to monitor low-temperature heteroepitaxial growth of $Ga_xIn_{1-x}P$ and GaP on Si during pulsed chemical beam epitaxy. RDS and PRS show that alternatively supplying V–III precursors results in a periodic change of the surface chemistry, which appears either as a periodic oscillation of the anisotropy as measured by RDS or as oscillations as measured by PRS. The response of the GaP surface to single TEG and TBP pulses shows that the TEG fragments on the surface have a tendency to form clusters (islands) of Ga, which are dispersed after TBP exposure. The modeling of the fine structure oscillations of the PRS signal show that PRS and

RDS are highly sensitive to a periodically created and consumed surface reaction layer during the pulsed supply of precursors.

Acknowledgements

This work is supported by the Alexander von Humboldt Foundation, the Office of Naval Research under contract N-00014-93-1-0255, and the DOD/AFOSR MURI Grant F49620-95-1-0447.

References

[1] K.P. Killeen and W.G. Breiland, J. Electron. Mater. 23 (1993) 179.
[2] H. Grothe and F.G. Boebel, J. Crystal Growth 127 (1993) 1010.
[3] D.E. Aspnes, W.E. Quinn and S. Gregory, J. Vac. Sci. Technol. A 9 (1991) 870.
[4] D.E. Aspnes, J.P. Harbison, A.A. Studna and L.T. Florez, Appl. Phys. Lett. 52 (1988) 957.
[5] D.E. Aspnes, J.P. Harbison, A.A. Studna, L.T. Florez and M.K. Kelly, J. Vac. Sci. Technol. A 6 (1988) 1327.
[6] N. Kobayashi and Y. Horikoshi, Jpn. J. Appl. Phys. 28 (1989) L1880.
[7] Y. Horikoshi, Progr. Crystal Growth Characterization Mater. 23 (1992) 73.
[8] D.E. Aspnes, W.E. Quinn and S. Gregory, Appl. Phys. Lett. 56 (1990) 2569.
[9] N. Dietz, A.E. Miller, J.T. Kelliher, D. Venables and K.J. Bachmann, J. Crystal Growth 150 (1995) 691.
[10] K.J. Bachmann, N. Dietz, A.E. Miller, D. Venables and J.T. Kelliher, J. Vac. Sci. Technol. A 13 (1995) 696.
[11] A.E. Miller, J.T. Kelliher, N. Dietz and K.J. Bachmann, Mater. Res. Soc. Symp. Proc. 355 (1995) 197.
[12] N. Dietz, A.E. Miller and K.J. Bachmann, J. Vac. Sci. Technol. A 13 (1995) 153.
[13] N. Dietz and K.J. Bachmann, Mater. Res. Soc. Bull. 20 (1995) 49.
[14] K.J. Bachmann, U. Rossow and N. Dietz, Mater. Sci. Eng. B 37 (1995) 472.
[15] N. Dietz, U. Rossow, D. Aspnes and K.J. Bachmann, J. Electron. Mater. 24 (1995) 1569.
[16] N. Dietz and K.J. Bachmann, Vacuum 47 (1996) 133.
[17] A.A. Studna, D.E. Aspnes, L.T. Florez, B.J. Wilkens and R.E. Ryan, J. Vac. Sci. Technol. A 7 (1989) 3291.
[18] D.F. Edwards, in: Handbook of Optical Constants, Ed. E.D. Palik (Academic Press, New York, 1985) p. 547.
[19] A. Borghesi and G. Guizzetti, in: Handbook of Optical Constants, Ed. E.D. Palik (Academic Press, New York, 1985) p. 445.
[20] U. Rossow and D.E. Aspnes, to be published.